13th International Conference on
Structural Health Monitoring of Intelligent Infrastructure
DOI: 10.3217/978-3-99161-057-1-026

Structural health monitoring in underground mining using fiber-optic sensing and 3D laser scanning for digital twin development

Michael Dieter Martin[1, 0009-0003-7881-6456], Nils Nöther[2], Jens-André Paffenholz[1, 0000-0003-1222-5568]
[1]Clausthal University of Technology, Institute of Geotechnology and Mineral Resources, Geomatics for Underground Systems, Erzstraße 18, 38678 Clausthal-Zellerfeld, Germany
[2]fibrisTerre Systems GmbH, Torellstraße 7, 10243 Berlin, Germany
email: michael.dieter.martin@tu-clausthal.de, nils.noether@fibristerre.de, jens-andre.paffenholz@tu-clausthal.de

ABSTRACT: This study aims to evaluate the use of distributed fiber-optic strain and temperature sensing for structural health monitoring in underground mining drifts and chambers including 3D mobile laser scanning. This method seeks to create a digital twin to improve safety and efficiency through better digital planning. Temperature and deformation data from distributed fiber-optic sensing (DFOS) cables will serve as boundary conditions of the combined ventilation and geomechanical models of the drift and chambers. Initially, a 60-meter-long drift will be monitored using fiber-optic cables. Next, deformations of a flexible arch support, induced by hydraulic cylinders, will be observed. A hydraulic cylinder will then apply load orthogonally to the rock. Fiber-optic cables will be inserted and cemented into the rock, along rock bolts, and in boreholes around each bolt to measure deformations from rock bolt pull-out tests. Preliminary examinations identified the best adhesive bonding method for DFOS cables, considering the specific ambient conditions. A 3D point cloud will be used to plan and validate the cable installation. The meshed 3D cloud will serve as the foundation for the combined ventilation and geomechanical models, creating a virtual reality-capable digital twin enhanced with live DFOS measurements.

KEY WORDS: fiber-optic sensing, 3D point cloud, digital twin, underground mining

1 INTRODUCTION

In the recent years, digital twins have increasingly been investigated within the realms of tunnel construction [1] and mining [2], [3] with promising results. All digital twins must be provided with real data to capture and model reality as closely as possible (e.g. [1], [3], [4]). Depending on the particular use of the digital twin, various types of datasets and sensors are used including 3D laser scanners, environmental data such as temperature and humidity [1] and information on geology and rock deformation [3] to name only a few. Since the beginning of modern fiber-optic development in the 1960s, distributed fiber-optic sensing (DFOS) has found a wide range of applications ranging from infrastructure health monitoring [5], [6], river dikes [7], volcano monitoring [8] and tunnel monitoring as well as underground mine monitoring [9], [10]. In the context of the latter, the DFOS technique enables the detection of small temperature and strain changes and their resulting deformations [9], [10]. In the realm of DFOS based measurement principles, the Brillouin optical frequency domain analysis (BOFDA) technique [11] allows for distributed measurements along several kilometers with a spatial resolution below 1-meter [7] and has been successfully used for structural health monitoring [5], river dike monitoring [7] and tunnel inspection [9].

In this paper, the BOFDA based fiber-optic solution provided by fibrisTerre Systems GmbH (Germany) is used. The mine used for installation of the fiber-optic cables and for construction of the underground lab is the research and education mine “Forschungs- und Lehrbergwerk (FLB) Reiche Zeche” at TU Bergakademie Freiberg (TUBAF) in Germany. The fiber-optic cables will be installed in a 60 m long drift and additionally in four chambers for experimental setups. Both the main drift and the chambers form part of the FLB mine and are referred to underground lab in the following. The first part of the installation of the fiber-optic cables is scheduled to be completed by September 2025.

The strain and temperature measurements will be used as boundary conditions for geomechanical and ventilation models, which will be coupled including a geometrical and geological model of the underground lab. The creation of an artificial intelligence (AI)-supported coupled model will enable real-time visualization of changes in physical parameters in the coupled geomechanical and ventilation model, which will ultimately lead to development of a digital twin**.** For a more detailed overview about the individual models see [12]. To our knowledge, fiber-optic sensing data was not yet used for providing temperature and strain measurements as boundary conditions for creating a digital twin in an underground mine. Therefore, the overall aim of the collaborative research project “MOdel coupling in the context of a VIrtual underground lab and its development process” (MOVIE) is to develop a digital twin of the underground lab provided with fiber-optic sensing-based temperature and strain data, which will ultimately be visualized using a Meta Quest 3 mixed-reality headset (see Figure 1).

DOI: 10.3217/978-3-99161-057-1-026

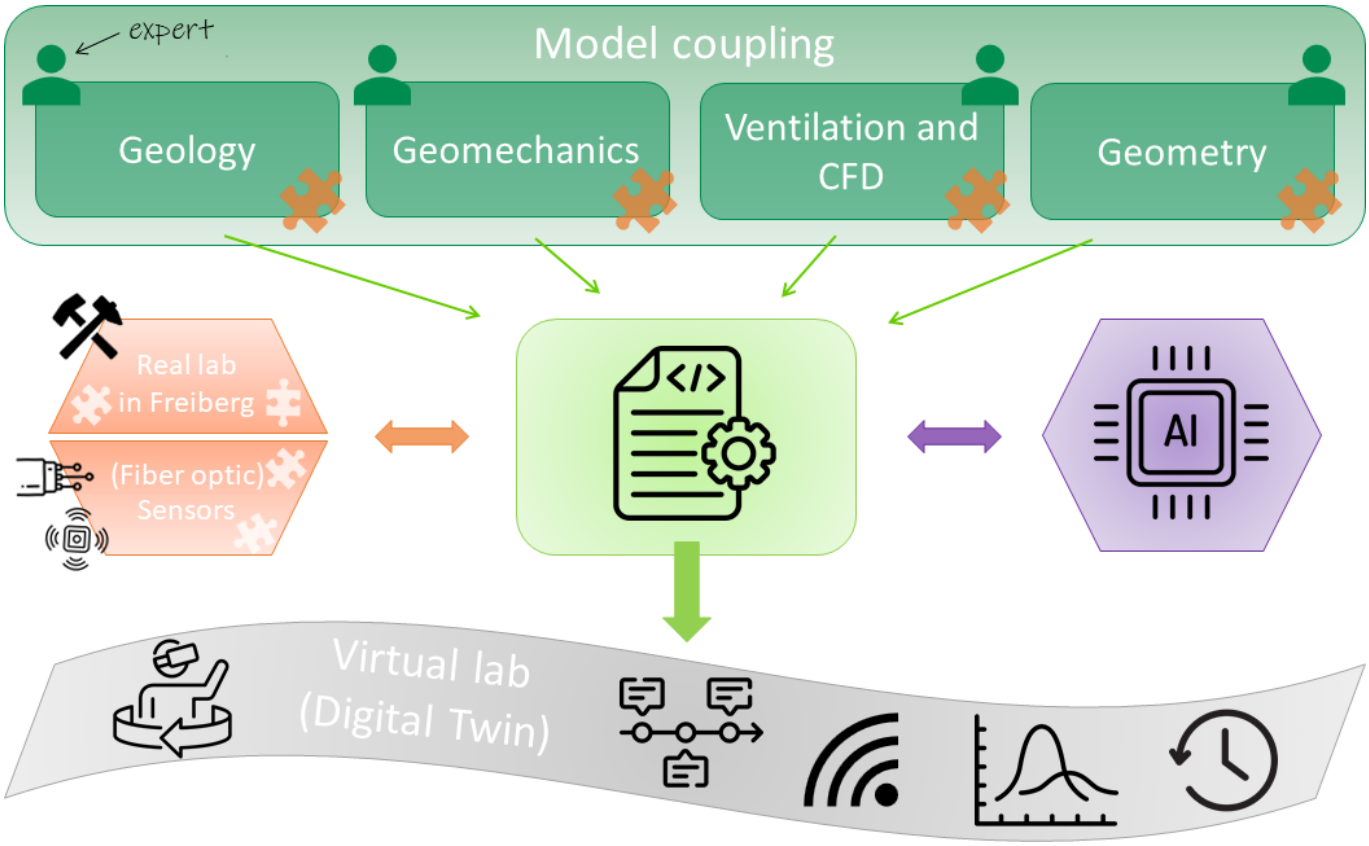

Figure 1 MOVIE project overview. Special emphasis in this paper is on fiber-optic sensing and laser scanning (Geometry).

The MOVIE project includes partners at five different departments at the Clausthal University of Technology (TUC) and one department at the TU Bergakademie Freiberg (TUBAF). Additionally, one external industry partner is included, fibrisTerre Systems GmbH (fibrisTerre). The project is led by the Chair of Geomatics for Underground Systems within the Institute of Geotechnology and Mineral Resources (IGMR) at the TUC. Despite the MOVIE project covering various aspects of geomechanical and ventilation modeling and AI application, this paper focuses on the installation of the fiber-optic cables, supported by a 3D point cloud acquired with a Zoller+Fröhlich (Z+F) FlexScan 22 mobile mapping SLAM platform. Additionally, the meshed surface of the underground lab, i.e., the geometrical model, generated from the 3D point cloud is of concern in this paper.

2 MATERIALS AND METHODS

2.1 The underground lab

Geologically, the FLB mine consists of ortho- and paragneisses and is veined with silver/lead/zinc mineralization. From the first discovery of silver-rich ores in 1168, active mining was maintained until 1969 with a focus on lead and zinc in the last exploitation stage [13]. Currently, the mine hosts more than 30 national and international collaborative research projects conducted in the underground space. The decision to plan the underground lab here is based on this particular part of the mine being relatively isolated from the other mine workings and experiments. The area of the underground lab can only be accessed via two raises from a lower level, however, only one of the raises has a mine ladder, while the other access is intended for material transport via winches. This isolated location allows the conditions to be well controlled, particularly in terms of temperature and ventilation. The underground lab (see Figure 5) consists of a 60 m long main drift and four chambers with variable roof heights ranging between 2.75 and 4.9 m.

2.2 3D point cloud acquisition and data processing

Two 3D point clouds of the underground lab were acquired in two different field campaigns using a Z+F FlexScan 22 mobile mapping SLAM platform (Figure 2). The first point cloud was acquired in March 2024 containing a total of 368,291,128 points (~9.75 GB in e57-format). The second point cloud was acquired in May 2024 containing a total of 621,441,614 points (~16.5 GB in e57-format). The Z+F FlexScan 22 system incorporates a Z+F IMAGER 5016a laser scanner mounted on a backpack, merging the high spatial resolution of a stationary laser scanner with the versatility of a mobile platform. This technology is based on the simultaneous localization and mapping (SLAM) approach, which enables to create a map of the environment while data capturing [14].

The acquired 3D point clouds were processed using the software Z+F Lasercontrol 10.0.7.1. including loop closure, intensity based filtering and manual cleaning of noisy data points. Additionally, the 3D point clouds were aligned and registered using the open-source software packages CloudCompare 2.13.2. In the next processing stage, the resulting aligned and registered 3D point cloud was meshed based on a Poisson-Surface reconstruction approach using the

DOI: 10.3217/978-3-99161-057-1-026

open-source software package MeshLab 2023.12 to generate triangular meshes with variable spatial resolutions. The generated mesh, i.e., the geometrical model, serves as the input to the geomechanical and ventilation models created by the project partners at TUC. Additionally, the geometrical model was visualized using the software package LiquidEarth One provided and developed by Terranigma Solutions GmbH. This software package was specifically designed for the visualization of geologic models in virtual reality including the use of a Meta Quest 3 VR headset and serves as the target software for visualization of the digital twin to be developed in the MOVIE project.

Figure 2 Z+F FlexScan22 mobile mapping SLAM platform.

2.3 Gluing experiments on fiber-optic cables using epoxy resin glue and injection mortar

The use of the fiber-optic cable type Fibrasens DSS-S and the fiber-optic cable type Solifos BRUsens DFOS B-DTS 2SMF was decided due to their specific design to perform strain and temperature measurements, respectively. Additionally, the cables have an overall good flexibility and proved to be reliable in former projects of fibrisTerre.

Especially for fiber-optic strain measurements, optimal bonding conditions to the object to be measured have to be ensured. Typically, DFOS cables for strain and temperature measurements are installed on pre-existing structures, e.g. in geotextiles [7], along rock bolts [10] or on reinforcement grids [9]. However, in the underground lab, none of these structures are present and installation along, e.g., rock bolts would result in a spatial discretization of the deformation measurement to the span interval between the rock bolts, e.g., [10]. Therefore, gluing experiments using the Fibrasens DSS-S strain cable were conducted on-site in the underground lab and under room temperature conditions in the Geomatics Indoor Lab at the IGMR using hand specimens taken from the underground lab to identify the optimal adhesive bonding method. Based on experiences of fibrisTerre, the epoxy resin glue Sikadur 31+ from Sika and the injection mortar FIS VS Low Speed 300 T from Fischer were tested. The Sikadur 31+ consists of two components that must be mixed in an external container before application. One container of the epoxy glue, containing a total of 1.2 kg, was used for the test. The epoxy glue is a moisture-tolerant adhesive designed to bond a variety of different materials including concrete, natural stone, ceramics etc. and is used for repairs, joint fillings and crack sealing. According to the manufacturer information [15] the Sikadur 31+ has a compressive strength of ~50 MPa and a tensile strength of ~6 MPa after 3 days curing time at +10°C. The shear strength is reported as ~16 MPa. In contrast, the FIS VS Low Speed 300 T is delivered in a cartridge press containing 490 g of two components that are instantly mixed in the press upon handling. This injection mortar has approved use in water-filled drill holes and is used for fixations in cracked and non-cracked concrete as well as masonry. Due to its preferred use with anchors in drill holes, the strength metrics of the FIS VS Low Speed 300 T depend on the diameter of the anchor/rod used and the composition of the concrete/masonry. Information on bonding strength metrics were taken from the manufacturer homepage [16]. According to manufacturer information, permissible tensile loads are in the order of 0.34 kN up to 3.43 kN and permissible shear loads are in the order of 0.26 kN to 3.28 kN for solid and perforated masonry. In normal concrete, values for permissible tension and shear loads ranging from 3.9 kN up to 121.2 kN are reported depending on the anchor/rod type used. The characteristics of the epoxy resin glue and the injection mortar were estimated to be suitable to securely bond the Fibrasens DSS-S cable with a weight of 9 kg/km to the gneiss host rock.

Handling and application were tested using both a cartridge press and a trowel. The behavior of both the epoxy glue and injection mortar under dry and wet surface conditions was tested. Before gluing a cable to the wall or the specimen, the surface was prepared using a scratch brush to remove loose particles and dust. For temporarily fixing the fiber-optic cable to the rock surface, two fabric tapes were tested. The first was a standard tape for domestic use, and the second was the natural rubber tape “Beton- und Mauerband Premium, 44 mm x 50m” specifically manufactured for use on poorly adhering surfaces such as walls and concrete [17].

2.4 The DFOS measurement system

The fiber-optic measurements presented in this paper are based on the DFOS principle, specifically using the BOFDA, which enables spatially resolved strain and temperature measurements along the profile of the fiber. The measurement hardware consists of an interrogation unit (model name: fTB 5020), a fiber-optic switch for channel extension (a total of 12 channels for this project), an industrial PC and an ethernet switch for internet connection (Figure 3). For data analysis, the software fTView will be used and the cloud platform fTScope for data storage (not shown in Figure 3).

The BOFDA measurement enables a range of spatial resolutions for temperature and strain measurements of 0.2 m to 2.5 m depending on the fiber length. The minimum resolvable event is >2 microstrain [με] and >0.1°C for temperature measurements. Total fiber lengths of up to 80 km are possible [18].

The BOFDA technique makes use of the so-called Brillouin frequency shift of the fiber, which in a first instance is dependent on the intrinsic properties of the fiber material itself. However, small changes in the local density also impact the Brillouin frequency shift, which are interpreted in terms of changes in temperature and strain [7].

DOI: 10.3217/978-3-99161-057-1-026

The conversion from Brillouin frequency shift [GHz] to temperature and strain for each position along the fiber is performed using the following relationships:

$$f_B = f_{B0} + \varepsilon \cdot c_\varepsilon \quad (1)$$

$$f_B = f_{B0} + (T - T_0) \cdot c_T \quad (2)$$

where f_B is the measured Brillouin frequency shift [GHz], T is the temperature [°C] and ε is the applied strain in microstrain [με]. The calibration parameters f_{B0}, c_ε and c_T are dependent on the specific optical fiber and cable type used (strain or temperature cable).

To test the DFOS measurement configuration, an aluminum frame was installed in the Geomatics Indoor Lab at the IGMR, which will be equipped with clamping jaws and deflection rolls to enable test strain and temperature measurements using both cable types.

2.5 *Fiber-optic cable installation configuration and experimental setup in the underground lab*

On-site in the underground lab, the fiber-optic sensors will be installed along the main drift to obtain longitudinal temperature and strain along the entire drift. These sensors will be installed with the aim of providing continuous measurements throughout the MOVIE project period. In contrast to the strain cable, the temperature cable in the main drift is planned to be installed disconnected from the drift wall using clamps, as measurements of the temperature of the air inside the drift is of interest. The temperatures on the surface of the rock, where the fiber-optic strain sensing cable is installed, are assumed to be overall stable and in equilibrium with air temperatures, with no sudden variations to be expected. The temperature distribution retrieved from the fiber-optic temperature sensing cable will therefore be suitable to temperature compensate the strain measurements along the drift, where the fiber-optic strain sensing cable is largely running in parallel to the temperature sensing cable. For the strain cable installations that are directed further into the gneiss body, being the rock bolt test installations, the temperature is assumed to be even more stable and constant over the cable length. The temperature impact on these strain measurements will therefore be neglected, and no temperature compensation is assumed to be necessary. To induce measurable deformation in the gneiss that is large enough to be used as boundary conditions for the geomechanical model, three test rigs will be installed in three of the four chambers to perform short-term push and pull experiments. In the first chamber, an arch support will be installed in such a way that a distance from direct contact with the rock is maintained, allowing exertion of pressure on specific points of the support structure. In the second chamber, a hydraulic cylinder will be installed, which enables to transfer a load orthogonally onto the rock.

For both chambers, stress and strain changes will be recorded with fiber-optic cables installed superficially either in the support structure of the arch or directly on the chamber wall surrounding the hydraulic cylinder.

In the third chamber, four separate configurations of 4 m long anchor boreholes surrounded by four 5 m long measurement boreholes are planned, resulting in a total of four anchor boreholes and 20 measurement boreholes to be drilled. The fiber-optic cables will be directly cemented into the rock along the rock bolts. For each of the four configurations separately, the rock bolt cemented in the anchor borehole will be pulled and deformations of the surrounding concrete and rock will be measured in the measurement boreholes along the cemented fiber-optic cables.

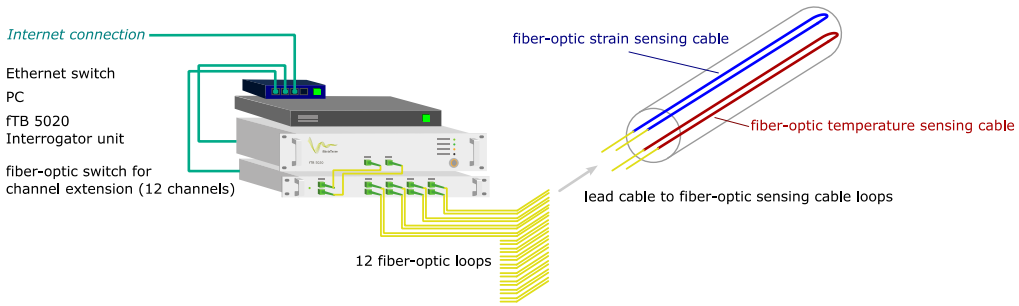

Figure 3 fibrisTerre measurement setup (principle).

Additional numerical simulations were conducted by the Geomechanics department at the TUC based on the rock elasticity modulus, the mechanical properties of the steel and the detection limit of the fibrisTerre interrogation unit of 2 με to ensure optimal fiber-optic cable installation planning. The simulation parameters are based on the dimensions of the planned experiments. For the hydraulic cylinder in chamber 2, a steel plate with diameters of 0,30 m was modeled, which was placed on a rock cube 1.5 m in diameter with an assumed elastic modulus of 50 GPa. A maximum pressure of 182 MPa was exerted on the steel plate. The simulation results were used to identify the maximum radius in which a superficial strain change can still be measured if a load is transferred onto the rock. Results showed a maximum radius of ~52 cm around the steel plate to be maintained for the cable installation (Figure 4). For the rock bolt pull out test in chamber 3, a borehole with a radius of 38 mm and a depth of 4 m was assumed, in which a rod with radius 25 mm and a length of 3975 mm is installed. The scenario was modeled under the assumption of inelastic grout and steel and a rock elasticity modulus of 50 GPa. The simulation results were used to identify the maximum distances between the anchor and measurement boreholes in which a strain change in the measurement borehole is expected to be still measurable. The results showed a maximum distance of ~36.2 cm to be maintained (Figure 4).

DOI: 10.3217/978-3-99161-057-1-026

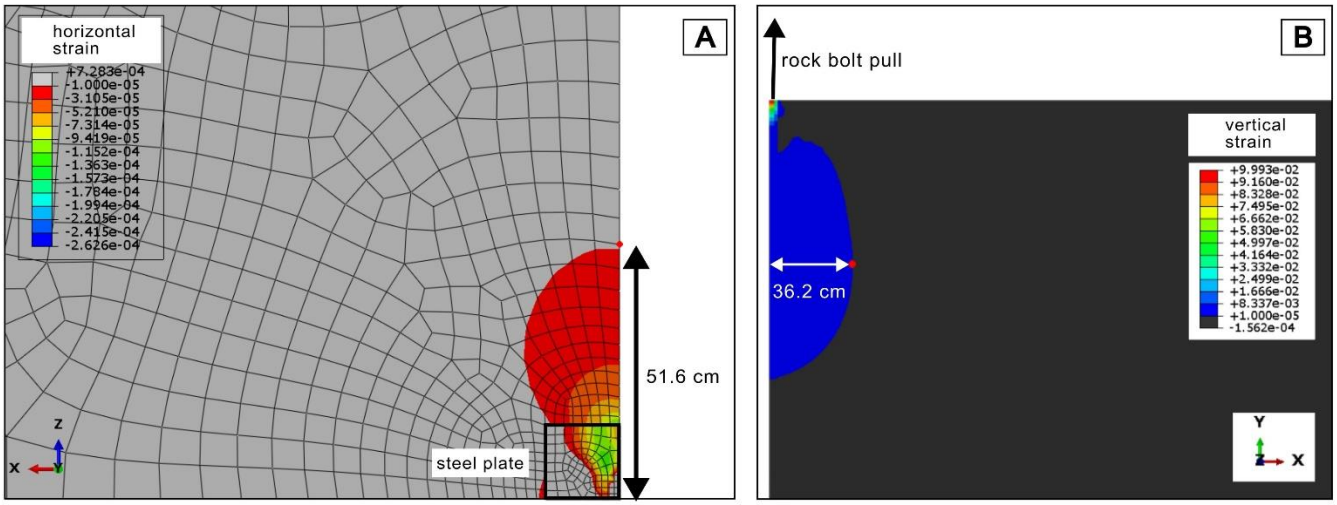

Figure 4 Geomechanical simulation results of (A) plate load test and (B) rock bolt pull out test. A strain cut off value of $10^{-5}$was used in both cases. To save computational effort and under the assumption of radial symmetry, only one fourth of the geometry was simulated.

The 3D point cloud acquired in May 2024 was used for fiber-optic cable installation planning for the main drift and the test rigs separately. The Trace Polyline tool available in the software package CloudCompare 2.13.2. was used to draw polylines in the 3D point cloud representing the fiber-optic cables to be installed. To estimate the overall lengths of the cables, the individual polylines were summed up in CloudCompare. Since the 3D point cloud only allows for estimating the lengths of cables installed superficially, the lengths of the cables needed for the rock bolts were added to the calculated superficial installation lengths.

All cables from the main drift installation and the test rigs will be installed in a loop configuration from and towards a fiber-optic cable termination box connected with the fibrisTerre measurement configuration, which both will be installed roughly opposite of chamber 2.

3 RESULTS

3.1 Visualization of 3D point cloud and determination of fiber-optic cable positions and their lengths

The 3D point cloud acquired in May 2024 was scanned with an average spatial resolution, i.e., average point distance, of approximately 0.76 mm in roughly 29.5 minutes. Due to computational performance reasons, a subsampled version of the original 3D point cloud with a resolution of ~3.63 mm (22,378,105 points; ~417 MB in .e57-format) was used for planning the installation of the fiber-optic cables, which still captured enough details to ensure realistic positioning of the cables. Figure 5 shows the subsampled 3D point cloud of the underground lab, including its four chambers. Additionally, Figure 5 shows the meshed 3D point cloud visualized in the target software for the digital twin LiquidEarth One. Figure 6 presents views within the 3D point cloud, showing the polylines representing the positions of the fiber-optic cables for the main drift and exemplary for chambers 1 and 2. Based on a high resolution meshed version of chamber 2, a relatively flat section extending across a large portion of the roof was identified, making it an ideal candidate for the installation of the hydraulic cylinder unit and the cables surrounding the terminating steel plate of the cylinder (see Figure 6C).

Table 1 Estimated lengths [in meters] of the Fibrasens strain cable and Solifos BRUsens temperature cable based on polylines drawn in the 3D point cloud

Position	**Experiment setup**	**Cable type**	**Length [m]**
Main drift	Continuous monitoring	Strain	138
Chamber 1	Arch support structure	Strain	29
Chamber 2	Hydraulic cylinder	Strain	35
Chamber 3	Rock bolt pull out	Strain	387
SUM [m]			**589**
Main drift	Continuous monitoring	Temperature	**138**

The lengths of the cables to be installed were determined in the 3D point cloud supported by the results of the geomechanical simulations. The overall length of the Fibrasens strain cable to be installed for the main drift and the test rigs was estimated to be roughly 600 m, while the overall length of the Solifos BRUsens temperature cable was estimated to be roughly 140 m. Table 1 presents the detailed estimated lengths for the strain cable along the main drift and the test rigs separately. Since temperature measurements are only performed along the main drift, the estimated length of the temperature cable is added at the bottom of Table 1.

DOI: 10.3217/978-3-99161-057-1-026

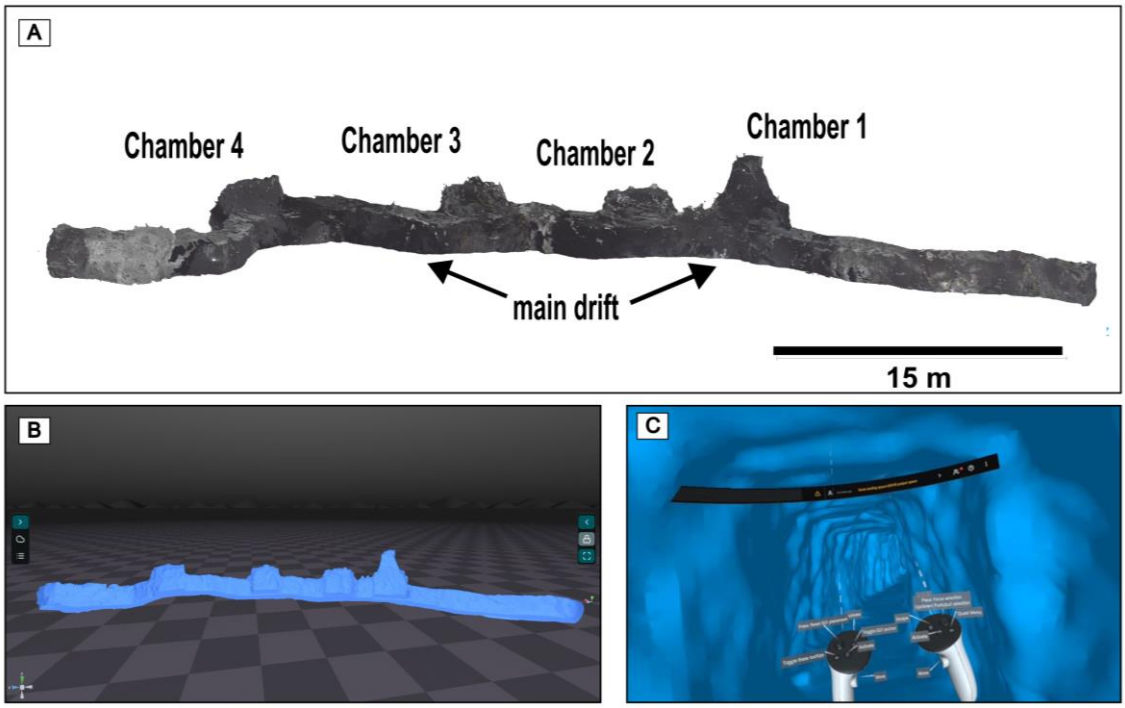

Figure 5 (A) 3D point cloud of underground lab including main drift and four chambers (chambers numbered 1 to 3 are used for installation of the test rigs); (B) Meshed 3D point cloud visualized in software LiquidEarth One developed by Terranigma Solutions GmbH; (C) View inside the underground lab in LiquidEarth One using a Meta Quest 3 VR headset.

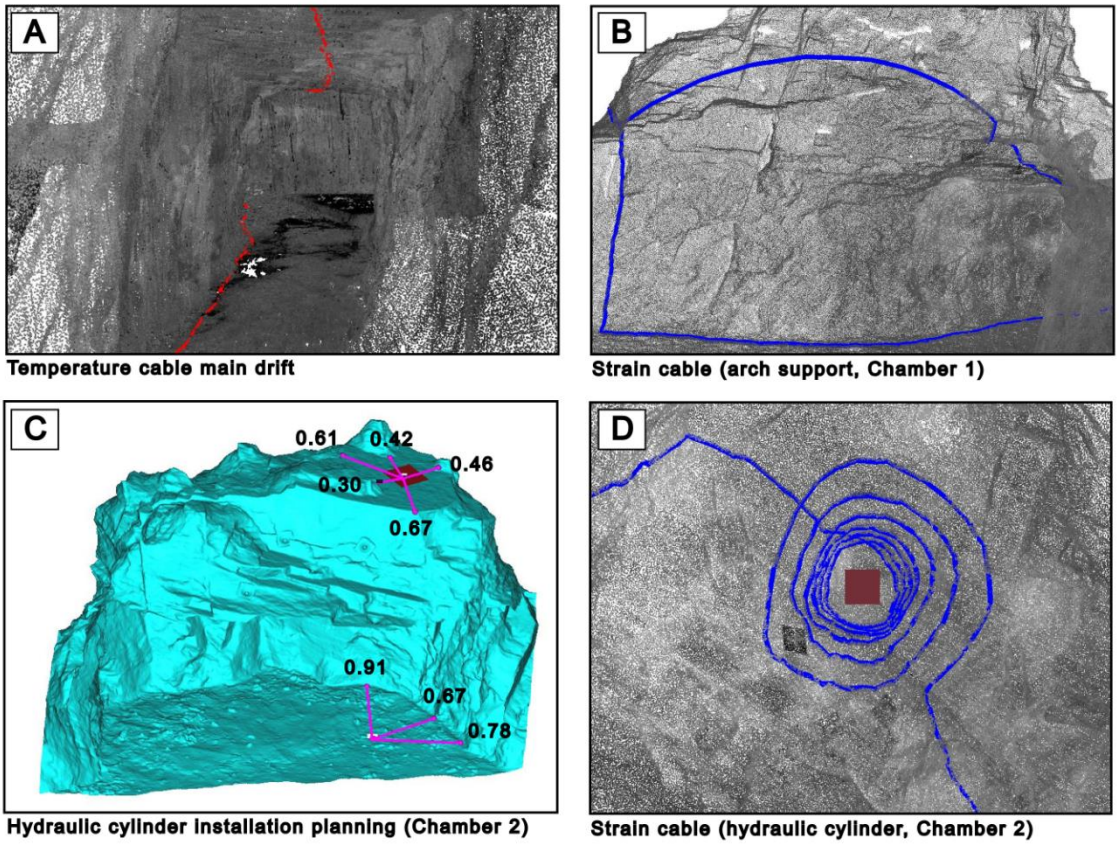

Figure 6: Views in the 3D point cloud (and mesh) showing the positions of the fiber-optic cables to be installed as polylines (A) BRUsens temperature cable in main drift, (B) Fibrasens strain cable in the arch support structure (Chamber 1), (C) Meshed 3D point cloud of Chamber 2 for estimation of distances (in meters) to the walls for installation planning of the hydraulic cylinder. The terminating steel plate of the hydraulic cylinder is shown as a dark red square on the chamber roof (D) Fibrasens strain cable around the steel plate of the hydraulic cylinder (dark red) in Chamber 2 (view towards the chamber roof)

DOI: 10.3217/978-3-99161-057-1-026

3.2 The gluing experiments

Several gluing tests were conducted to ensure optimal bonding between the Fibrasens strain cable and the drift wall (Figure 7). For temporarily fixing the cable to the rock surface, the tape for domestic-use did not provide sufficient adhesion for both dry and wet surfaces. However, the special wall and concrete tape adhered well to a dry surface. Under room temperature conditions in the Geomatics Indoor Lab at IGMR, the Sikadur 31+ epoxy resin glue achieved its maximum bonding strength one day after application, with no observable differences for wet and dry surfaces. After mixing, the epoxy resin glue remained usable for approximately 60-70 min, but became sticky (and therefore unworkable) after roughly 90 min. Once applied, the cables were securely fixed to a rock specimen in the Geomatics Indoor Lab or on-site on the drift wall and could not be removed by pulling on the cable. In contrast, the FIS VS Low Speed 300 T injection mortar reached maximum bonding strength after just 3.5-5 min. However, on damp surfaces, the cured mortar broke off with slight force. Application of both the glue and the mortar to a vertical wall and overhead was challenging, as a lot of material crumbled or fell off and did not adhere to the rock. The use of a cartridge press and a trowel partially solved this problem and proved to be the most effective method to best apply both the glue and the mortar to the rock.

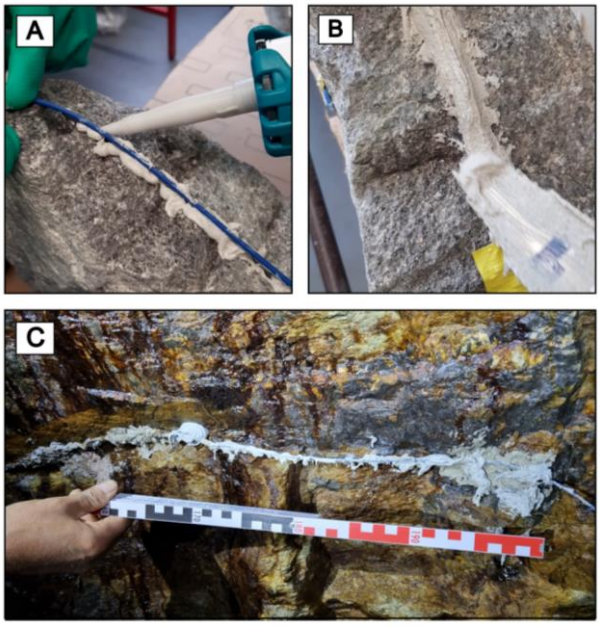

Figure 7 Gluing tests with Fibrasens strain cable on a hand specimen (A) using a cartridge press and (B) a trowel; (C) Fibrasens strain cable glued to drift wall on-site in the underground lab (measuring rod for scale)

4 DISCUSSION

4.1 3D mobile laser scanning and determination of fiber-optic cable positions/lengths

The Z+F FlexScan22 mobile backpack laser scanner solution proved capable of accurately capturing the complex wall geometry of the underground lab with a very high resolution of approximately 0.76 mm in about 29.5 min acquisition time. Compared to a classical terrestrial laser scanning system, at least about eight different stationary scanner positions would have been necessary to capture the underground lab, resulting in a much longer data acquisition time. Despite the high data acquisition speed, a shortcoming of the mobile laser scanning system are omnipresent noise pixels in the drift, which requires greater (manual) cleaning efforts compared to data acquired with a stationary terrestrial laser scanner system. In contrast, the registration of independently acquired 3D point clouds is not necessary when using a mobile laser scanner system, which should result in an overall shorter time for data acquisition and processing using the Z+F FlexScan22 solution.

Using this approach made it possible to identify optimal positions for the fiber-optic cables and to estimate their required lengths in the 3D point cloud. Due to the high point density, it is not possible to click every successive point in the 3D point cloud as a vertex point of the polyline. This might lead to some of the distances between individual vertex points being shorter than in reality, since some of the line segments between individual vertex points might not follow the wall roughness, which might result in a slight underestimation of the cable lengths. Conversely, due to uncertainties in the distance measurements themselves stemming from intrinsic device errors and external factors such as dust particles and/or humidity, the points in the 3D point cloud are slightly spread, i.e., not exactly matching with their position on the wall. This might lead to greater roughness in the 3D point cloud compared to the drift wall, which could, in contrast, result in a slight overestimation of the cable lengths. However, for the practical installation of the cables on-site, the estimated positions and cable lengths will act as a guiding principle and do not need to be accurate on a centimeter-scale. Additionally, the practical installation of the cables requires consideration of the maximum allowed bending radii, which are 3.8 cm for the Fibrasens strain cable and 9.6 cm for the Solifos BRUsens temperature cable. Due to the large roughness of the drift walls, the bending radii might be exceeded in some places particularly for the strain cable.

4.2 The gluing experiments and fiber-optic cable installation configuration

The Geomatics Indoor Lab and on-site experiments presented in this paper showed that gluing the strain cable to the drift wall is a difficult task, since most of the glue and mortar crumbles or falls off especially when working on a perpendicular wall or overhead. Still, direct installation on the wall is necessary in this project, since there are no pre-existing structures present in the underground lab, which the cable can be installed at and direct installation on the wall allows to make full use of the system's spatial resolution. To overcome this issue, cutting a ~3-25 mm deep and ~4 mm wide slit in the drift wall is planned with the strain cables placed in. After its installation, the slit will be closed with the injection mortar due to its easier handling and the shorter setting time if compared to the epoxy resin glue. Before application of the mortar, the acquisition of another 3D point cloud is planned to document the position of the slit (and therefore the position of the fiber-optic cable).

DOI: 10.3217/978-3-99161-057-1-026

The overhead installation of the cables might still be challenging, but could be successfully addressed with combined use of the cartridge press and trowel. If needed, "modeling" rough parts using the injection mortar is possible, which will ensure optimum bonding between the strain cables and the drift wall. Cable installation within the arch support structure and installation along the rock bolts for the rock bolt pull out test requires a different setup, which is in the planning phase at the time of writing this paper.

The current fiber-optic cable setup plans the installation of a termination box and the fibrisTerre measurement configuration in the underground laboratory. This results in the shortest possible spanned distances between the termination box and the individual test rigs (see Table 1). The same applies for the temperature and strain cables installed in the main drift for continuous measurements. Still, the planned setup in chamber 3 requires longer cable lengths if compared to the installations in chamber 1 and 2 due to cable installation along the 4 to 5 m long rock bolts. Additionally, each of the four configurations of anchor and measurement boreholes must be connected to the termination box separately, as the cable will most likely be destroyed after performing a pull out test. Besides pure cable installation with the help of a 3D point cloud, meshes were created for visualization purposes and a highly resolved mesh of chamber 2 was used for installation planning of the hydraulic cylinder. The mesh allowed to identify a region most suitable for installation of the terminating steel plate and to precisely determine the distances to the wall to ensure enough space for installation of the cylinder foot.

It is planned to prepare the cables based on the determined lengths in the Geomatics Indoor Lab at IGMR before installing them in the underground lab. This preparatory step might be beneficial, since the very sensitive splicing work should be kept away from the harsh and dark environment of an underground environment.

4.3 Long-term stability of the BOFDA measurement system

Due to its primarily measured material parameter being the intrinsic density of the optical fiber, the BOFDA technology is specifically long-term stable and free from the requirement of on-site sensor calibration both at the initial baseline measurements and during long-term operation. With the above calibration parameters known for the fiber-optic sensing cables in use (to be acquired from one-time lab tests), the Brillouin frequency shift from each measurement iteration can be converted into absolute values for temperature and strain, with no drift being caused by aging, fatigue, or changes in the optical properties of the cables and connectors. Therefore, the technique is especially suitable for the monitoring of the underground structure over a time horizon of many years. More critical, however, will be the long-term behavior of the bonding between the fiber-optic strain sensing cable and the rock and grout structures under test.

4.4 Preparation of data fusion and comparison to El Teniente mine (Chile)

A first attempt at fusing the fiber-optic position data, i.e., the polylines, with the BOFDA strain and temperature measurements provided promising results via exporting the strain and temperature data from fTView and merging them with the exported fiber-optic position data from CloudCompare using a Python script. When merged, the strain and temperature data can be re-loaded into CloudCompare as scalar fields of the position data and can be visualized. The strain and temperature measurements will serve as the boundary conditions for a coupled geomechanical and ventilation model provided by our project partners. As a first step towards visualization, the meshed version of the acquired 3D point cloud, i.e., the geometrical model, was uploaded and visualized in the target software for our digital twin LiquidEarth One using a Meta Quest 3 VR headset. The final product, i.e., the digital twin, to be visualized in LiquidEarth One and using virtual reality will be a coupled geomechanical and ventilation model provided with measurements from the fiber-optic sensors as boundary conditions and speeded-up with AI to shorten processing times and to enable real-time user interaction. The planned AI based approach is currently developed at TUC and is based on the Equilibrium Neural Operator (EquiNO) for solving steady-state multiscale modeling problems [19]. The expected results of the MOVIE project might be transferable to active mining environments such as e.g. the El Teniente mine in Chile. In this mine, fiber-optic sensors were installed in the ventilation level of a 201 m long test field and measured deformations were interpreted in terms of mining activities conducted in the production level [10]. The results presented in this paper are expected to be transferable to mines in a hard rock setting, such as e.g., the El Teniente mine [cf. [20]]. Additionally, the use of a digital twin, as described in this paper, might simulate the impacts of mining activities in terms of geotechnical parameters and ventilation even before a particular mine is opened, thereby enhancing safety and efficiency. Due to the capability of the BOFDA technology to measure within a range of up to 80 km, the results of this project should also be scalable to large mining areas. However, challenges remain in installing and protecting fiber-optic strain sensing cables when considering the occurrence of (locally constrained) deformations in the macrostrain region, such as e.g., in coal mines [21]. With both metallic and non-metallic fiber-optic sensing cable designs being typically specified for operation up to 1% strain, other strategies than straight gluing and pre-strained anchoring will need to be considered.

Since this is an ongoing research project, future changes to the described configurations and workflows might apply. Nevertheless, the results presented show the great potential of using 3D mobile laser scanning data for installation planning of fiber-optic cables in the underground space.

CONCLUSION

This paper presents the current state of the work done within the larger collaborative research project MOVIE with the aim of developing a digital twin of a 60 m long underground lab located in the FLB research mine in Freiberg (Germany) including real-time DFOS based temperature and strain measurements and visualization in VR. The installation planning of the fiber-optic cables was supported by SLAM based mobile laser scanning using a Z+F FlexScan 22

DOI: 10.3217/978-3-99161-057-1-026

platform. The acquired 3D point cloud was successfully used to estimate the lengths of the fiber-optic strain and temperature cables to be installed for both a continuous measurement setup and additional temporary experimental setups. Additionally, a meshed version of the 3D point cloud, i.e., the geometrical model, was visualized in virtual reality using a Meta Quest 3 VR headset. Since no pre-existing structures are present in the underground lab, several gluing tests under dry and wet conditions using the epoxy resin glue Sikadur 31+ from Sika and the injection mortar FIS VS Low Speed 300 T from Fischer were conducted. Overall, the injection mortar outperformed the epoxy resin glue due to its shorter setting time and easier handling and application. Future steps in the project will include installation of the strain cables in a slit cut in the drift wall and subsequent gluing with the injection mortar, which will enable a safe installation of the cables. An additional 3D point cloud will be acquired to document the positions of the cables once installed. The results of the DFOS temperature and strain measurements will be used as boundary conditions for a coupled geomechanical and ventilation model, which is supported with an AI model to enable real-time visualization of changes in physical parameters.

5 ACKNOWLEDGMENTS

The project "MOdellkopplung im Kontext eines VIrtuellen Untertagelabors und dessen Entwicklung-sprozess - MOVIE" is part of the research program "GEO:N - Geosciences for Sustainability" on the topic "Digital Geosystems: Virtual Methods and Digital Tools for Geoscientific Applications" funded by the German Federal Ministry of Research, Technology and Space (BMFTR). GEO:N is thus part of the BMFTR program "Research for Sustainable Development (FONA)". For the opportunity to realize this project, the consortium thanks the BMFTR and the project management organization.
[Reference: 03G0921A/ 2024-01 till 2026-12]

6 REFERENCES

[1] Z. Ye *et al.*, “A digital twin approach for tunnel construction safety early warning and management,” *Computers in Industry*, vol. 144, p. 103783, Jan. 2023, doi: 10.1016/j.compind.2022.103783.

[2] H. Gong, D. Su, S. Zeng, and X. Chen, “Advancements in digital twin modeling for underground spaces and lightweight geometric modeling technologies,” *Automation in Construction*, vol. 165, p. 105578, Sept. 2024, doi: 10.1016/j.autcon.2024.105578.

[3] M. Ghahramanieisalou and J. Sattarvand, “Digital Twins and the Mining Industry,” in *Technologies in Mining [Working Title]*, IntechOpen, 2024. doi: 10.5772/intechopen.1005162.

[4] F.-J. Kahlen, S. Flumerfelt, and A. Alves, Eds., *Transdisciplinary Perspectives on Complex Systems: New Findings and Approaches*. Cham: Springer International Publishing, 2017. doi: 10.1007/978-3-319-38756-7.

[5] K. Krebber *et al.*, “Structural Health Monitoring by Distributed Fiber Optic Sensors Embedded into Technical Textiles,” *tm - Technisches Messen*, vol. 79, no. 7–8, pp. 337–347, Aug. 2012, doi: 10.1524/teme.2012.0238.

[6] J. M. Lopez-Higuera, L. Rodriguez Cobo, A. Quintela Incera, and A. Cobo, “Fiber Optic Sensors in Structural Health Monitoring,” *J. Lightwave Technol.*, vol. 29, no. 4, pp. 587–608, Feb. 2011, doi: 10.1109/JLT.2011.2106479.

[7] N. Nöther, *Distributed fiber sensors in river embankments: advancing and implementing the Brillouin optical frequency domain analysis*. in BAM-Dissertationsreihe, no. 64. Berlin: Bundesanstalt für Materialforschung und -prüfung (BAM), 2010.

[8] P. Jousset *et al.*, “Fiber optic sensing for volcano monitoring and imaging volcanic processes,” May 05, 2024, *Physical Sciences and Mathematics*. doi: 10.31223/X5HM6J.

[9] F. Buchmayer, C. M. Monsberger, and W. Lienhart, “Advantages of tunnel monitoring using distributed fibre optic sensing,” *Journal of Applied Geodesy*, vol. 15, no. 1, pp. 1–12, Jan. 2021, doi: 10.1515/jag-2019-0065.

[10] H. Naruse *et al.*, “Application of a distributed fibre optic strain sensing system to monitoring changes in the state of an underground mine,” *Meas. Sci. Technol.*, vol. 18, no. 10, pp. 3202–3210, Oct. 2007, doi: 10.1088/0957-0233/18/10/S23.

[11] D. Garcus, T. Gogolla, K. Krebber, and F. Schliep, “Brillouin optical-fiber frequency-domain analysis for distributed temperature and strain measurements,” *J. Lightwave Technol.*, vol. 15, no. 4, pp. 654–662, Apr. 1997, doi: 10.1109/50.566687.

[12] E. Farys *et al.*, “Concept of a Digital Twin for an Underground Laboratory at the Reiche Zeche Mine Utilizing Artificial Intelligence,” in *2025 Preprints*, Colorado (USA): Society for Mining, Metallurgy & Exploration (SME), Feb. 2025, pp. 199–208. [Online]. Available: https://store.smenet.org/23c8kse#_=_

[13] J. Ostendorf, F. Henjes-Kunst, T. Seifert, and J. Gutzmer, “Age and genesis of polymetallic veins in the Freiberg district, Erzgebirge, Germany: constraints from radiogenic isotopes,” *Miner Deposita*, vol. 54, no. 2, pp. 217–236, Feb. 2019, doi: 10.1007/s00126-018-0841-1.

[14] H. Taheri and Z. C. Xia, “SLAM; definition and evolution,” *Engineering Applications of Artificial Intelligence*, vol. 97, p. 104032, Jan. 2021, doi: 10.1016/j.engappai.2020.104032.

[15] “Sikadur®-31+.” Accessed: June 30, 2025. [Online]. Available: https://industry.sika.com/en/home/renewable-energies/wind-energy/concrete-tower/structural-bonding/sikadur-31.html

[16] “fischer Injection mortar FIS VS Plus 300 T.” Accessed: June 30, 2025. [Online]. Available: https://www.fischer-international.com/en/products/chemical-fixings/injection-mortar/injection-mortar-fis-v-plus

[17] “Beton- und Mauerband Premium, 44 mm x 50 m Farbe: gelb kaufen Farbe: gelb.” Accessed: June 30, 2025. [Online]. Available: https://www.hygi.de/beton-und-mauerband-premium-44-mm-x-50-m-farbe-gelb-pd-125091

[18] fibrisTerre Systems GmbH, “fTB 5020 - Product Brochure.” 2019. [Online]. Available: https://www.fibristerre.de/file_download/15/fTB+5020+-+Product+Brochure.pdf

[19] H. Eivazi, J.-A. Tröger, S. Wittek, S. Hartmann, and A. Rausch, “EquiNO: A Physics-Informed Neural Operator for Multiscale Simulations,” Apr. 25, 2025, *arXiv*: arXiv:2504.07976. doi: 10.48550/arXiv.2504.07976.

[20] J. Cannell, D. R. Cooke, J. L. Walshe, and H. Stein, “Geology, Mineralization, Alteration, and Structural Evolution of the El Teniente Porphyry Cu-Mo Deposit,” *Economic Geology*, vol. 100, no. 5, pp. 979–1003, Aug. 2005, doi: 10.2113/gsecongeo.100.5.979.

[21] H. Gong, M. S. Kizil, Z. Chen, M. Amanzadeh, B. Yang, and S. M. Aminossadati, “Advances in fibre optic based geotechnical monitoring systems for underground excavations,” *International Journal of Mining Science and Technology*, vol. 29, no. 2, pp. 229–238, Mar. 2019, doi: 10.1016/j.ijmst.2018.06.007.